

## Adsorption and Dynamics of a Single Polyelectrolyte Chain near a Planar Charged Surface: Molecular Dynamics Simulations with Explicit Solvent

Govardhan Reddy,<sup>†</sup> Rakwoo Chang,<sup>‡</sup> and Arun Yethiraj<sup>\*,†</sup>

*Department of Chemistry, University of Wisconsin, Madison, Wisconsin 53706, and  
Department of Chemistry, Kwangwoon University, Seoul, 139-701, Republic of Korea*

Received October 27, 2005

**Abstract:** The effect of solvent quality on the behavior of a polyelectrolyte chain near a charged surface is studied using molecular dynamics simulation with explicit solvent. The polyion adsorbs completely on the surface for a high enough surface charge density, and the surface charge required for complete adsorption becomes lower as the solvent quality is decreased. Several static and dynamic properties display a nonmonotonic dependence on surface charge density and solvent quality. For a given value of solvent quality the component of the radius of gyration ( $R_g$ ) parallel to the surface is a nonmonotonic function of the surface charge density, and for a given surface charge density the component of  $R_g$  perpendicular to the surface is a nonmonotonic function of the solvent quality. The center-of-mass diffusion coefficient and rotational relaxation time are nonmonotonic functions of the surface charge density. Translational diffusion coefficient increases, and the rotational relaxation time decreases as solvent quality is decreased for a fixed surface charge density.

### I. Introduction

The ease of processing makes polymers useful coating materials. An intriguing case is when the polymer molecules contain charged groups along a hydrophobic backbone<sup>1–3</sup> because the balance between hydrophobic and electrostatic interactions can, in principle, be exploited to tune the adsorption and conformational properties. Charged polymers have a number of applications, for example, in electrooptic devices, semiconducting films, and drug delivery. Our understanding of the behavior of adsorbed polyions is not yet complete, however, and this is a problem of current interest.<sup>4</sup> In this work we study the adsorption of a charged polymer to an oppositely charged surface using molecular dynamics simulations.

There is a large body of theoretical and computational work on the adsorption of charged polymers to surfaces. These include scaling and meanfield theories for dilute<sup>5–17</sup> and semidilute<sup>10,12,13,16–25</sup> solution, and computer simulations

using Monte Carlo<sup>26–40</sup> and molecular dynamics<sup>41–44</sup> methods. There has been much less attention, in computer simulations, on the effect of solvent quality on polyion adsorption. Since in many cases, e.g. polystyrene sulfonate, the polyions are composed of hydrophobic backbones for which water is a bad solvent, the effect of solvent quality can be important. In fact, it is often suggested that the solvent plays a crucial role<sup>45–47</sup> in the polyion adsorption on surfaces.

In the theoretical study of polymeric materials some level of coarse-graining in the model is necessary, given the size of the molecules. This is particularly true of charged polymers because the molecules can be significantly stretched. Several levels of coarse-graining are possible. At the united atom level a small group of atoms, e.g.,  $\text{CH}_2$  in polyethylene, is treated as a single site. This model preserves the carbon–carbon bond angle and bond length characteristics but coarse grains over hydrogen atoms. A more computationally convenient model, which has played an important role in our understanding of polymer solutions and melts, is when several of these united atoms are treated as a single site. This results in a class of models that can be loosely referred

\* Corresponding author e-mail: yethiraj@chem.wisc.edu.

<sup>†</sup> University of Wisconsin.

<sup>‡</sup> Kwangwoon University.

to as bead-spring models, an example of which is the freely jointed tangent hard sphere model. Information about local chemical details is lost in this class of models, but they provide a computationally convenient way of investigating the effect of parameters, for example the degree of polymerization, on the physical properties.

In the study of polymer solutions, the properties of the solvent molecules are generally not of interest, and it is attractive to be able to coarse-grain out the solvent coordinates. The result is an effective solvent-induced potential between polymer sites. A further approximation is to assume that this potential is pairwise additive. For polymers in poor solvents, i.e., when the polymer–solvent interactions are not favorable, the solvent-induced interaction is attractive in nature and tends to collapse the chain for sufficiently strong solvent-induced interactions. Note that in general this solvation potential should be many-body in nature, as is clear from the McMillan-Mayer theory,<sup>48</sup> and a pairwise additive form can never be exact.

The treatment of the solvent can play an important role in simulations of polymers in poor solvents. When the polymer chain is collapsed, the solvent is excluded from the globule to a large extent. In simulations with explicit solvent, the interactions between the interior polymer sites is just a weak van der Waals attraction between the hydrocarbon sites. With a pairwise additive implicit solvent, however, there is a very strong attraction between these interior sites which artificially increases the stability of the globule. The physical origin of this effect is that a potential, which is appropriate for two isolated monomers in the solvent, has been used under conditions where there is no solvent present. The consequence is that simulations of polymers in poor solvents often get trapped in meta-stable states unlike corresponding simulations with explicit solvent. In fact, the collapse dynamics of a homopolymer<sup>49</sup> and the phase behavior of polyelectrolyte solutions<sup>50</sup> are *qualitatively* different in pairwise additive implicit solvent simulations, when compared to explicit solvent simulations.

In this work we study the role of the solvent on the properties of a single polyion adsorbed on a planar surface using computer simulations. We include the solvent explicitly and perform molecular dynamics simulations on a system composed of a polyion, counterions, co-ions (counterions to the surface), and solvent particles, confined between two surfaces. The polyion is composed of freely jointed hard spheres with a negative charge on each sphere and the surface as atomically smooth with a uniform positive charge spread. The counterions to the polyion and the co-ions (ions which balance the charge on the surface) are monovalent hard spheres with positive and negative charges, respectively.

We find that the polyion adsorbs completely (flat) onto the surface for sufficiently high surface charge densities or poor enough solvents. Several static and dynamic properties have a nonmonotonic dependence of surface charge density and solvent quality. For example, the component of the radius of gyration parallel to the surface, the center-of-mass diffusion coefficient, and the rotational relaxation time show a nonmonotonic dependence on the surface charge density (for a given quality of solvent), while the component of the

radius of gyration perpendicular to the surface shows a nonmonotonic dependence on solvent quality. In all cases the chain center-of-mass exhibits normal diffusive behavior, but in good solvents the end-to-end vector autocorrelation function does not decay over the course of the simulation. Interestingly the chain dynamics become faster as the solvent quality is decreased.

The rest of the paper is organized as follows. The molecular model and simulation details are presented in section II, results are presented and discussed in section III, and some conclusions are presented in section IV.

## II. Molecular Dynamics Simulations

**A. Molecular Model.** The molecular model is similar to the model used by Chang and Yethiraj<sup>50</sup> in their study of polyelectrolytes in poor solvents. The polyion is modeled as a flexible bead spring chain composed of monomers with one negative charge each, and the counterions to the polyion are monovalent positively charged spheres. The charged surface is modeled as atomically smooth with a uniform positive surface charge density. The co-ions (which balance the surface charge) are monovalent negatively charged spheres. Solvent molecules are incorporated explicitly and are modeled as uncharged spheres.

The potential of interaction  $V_{ij}(r)$  between any two particles  $i$  and  $j$  is given by the sum of an electrostatic and nonelectrostatic part, i.e.,

$$V_{ij}(r) = k_B T \frac{q_i q_j \lambda_B}{r} + \lambda_{ij} V_{LJ}(r) + (1 - \lambda_{ij}) V_{WCA}(r) \quad (1)$$

where  $k_B$  is the Boltzmann's constant,  $T$  is the temperature,  $q_i$  is the charge valence of site  $i$ ,  $\lambda_B \equiv e^2/\epsilon k_B T$  is the Bjerrum length,  $e$  is the electronic charge,  $\epsilon$  is the dielectric constant of the solvent, and the parameters  $\lambda_{ij}$  control the quality of the solvent. The potentials  $V_{LJ}(r)$  and  $V_{WCA}(r)$  are the full and purely repulsive Lennard-Jones (LJ) potentials, respectively, and are given by

$$V_{LJ}(r) = \begin{cases} 4\epsilon_{LJ} \left[ \left( \frac{\sigma}{r} \right)^{12} - \left( \frac{\sigma}{r} \right)^6 - c(2.5\sigma) \right] & r \leq 2.5\sigma, \\ 0 & r > 2.5\sigma, \end{cases} \quad (2)$$

and

$$V_{WCA}(r) = \begin{cases} 4\epsilon_{LJ} \left[ \left( \frac{\sigma}{r} \right)^{12} - \left( \frac{\sigma}{r} \right)^6 - c(2^{1/6}\sigma) \right] & r \leq 2^{1/6}\sigma, \\ 0 & r > 2^{1/6}\sigma, \end{cases} \quad (3)$$

where  $\epsilon_{LJ}$  is the attractive well depth, and the function  $c(r)$  is chosen such that the value of the potential is zero at the cutoff, i.e.,  $c(r) = (\sigma/r)^{12} - (\sigma/r)^6$ .

The  $\lambda_{ij}$  parameters determine the quality of the solvent. In this work, we set  $\lambda_{mm} = \lambda_{ss} = \lambda$ , where m denotes monomer and s denotes solvent, and  $\lambda_{ij} = 0$  for all other pairs of  $i$  and  $j$ . The nonelectrostatic contribution to the potential to all the pairs is purely repulsive except for the monomer–monomer and solvent–solvent interactions. The parameter  $\lambda$  introduces an attractive well depth between monomer–monomer and solvent–solvent interactions as it is increased from 0 to 1. When  $\lambda = 0$ , all nonelectrostatic interactions are identical, and therefore the solvent quality

is good. On the other hand, when  $\lambda$  is large and positive the attractions between monomers and between the solvent molecules makes the solvent quality poor.

The nonelectrostatic interaction between the particles and the surface is purely repulsive and is given by<sup>51</sup>

$$V_{\text{wall}} = \begin{cases} 2\pi\epsilon_w\sigma_w^2 \left[ \frac{2}{5} \left( \frac{\sigma_w}{z} \right)^{10} - \left( \frac{\sigma_w}{z} \right)^4 + \frac{3}{5} \right] & z \leq \sigma_w, \\ 0 & z > \sigma_w, \end{cases} \quad (4)$$

where  $z$  is the perpendicular distance from the particle to the solid surface and the subscript  $w$  denotes the surface. This potential is obtained from the integration of the 12–6 LJ potential of a planar solid continuum in the two directions parallel to the surface. We set  $\epsilon_w = \epsilon_{\text{LJ}}$  and  $\sigma_w = \sigma$  for all the particles present in the simulation box. Both the surfaces interact with the particles in the simulation cell using the soft core repulsive LJ potential given by eq 4, but only one of the surfaces is electrically charged. The electric field,  $E_j$ , acting on a charged particle  $j$  due to the uniform charge density,  $\sigma_{\text{SCD}}$ , on a nonconducting surface is given<sup>52</sup> by  $E_j = (\sigma_{\text{SCD}}/2\epsilon)$ , and the direction of  $E_j$  is perpendicular to the surface.

The bonding potential between neighboring beads in the polyion is given by the FENE (finitely extensible nonlinear elastic) potential<sup>53</sup>

$$V_{\text{FENE}}(r) = -\frac{1}{2}k_{\text{FENE}}R_o^2 \ln \left( 1 - \frac{r^2}{R_o^2} \right) \quad (5)$$

where  $k_{\text{FENE}}$  is the spring constant and  $R_o$  is the maximum extension of the bond. In this work, we set  $k_{\text{FENE}} = 30.0k_B T/\sigma^2$  and  $R_o = 1.5\sigma$ ; these parameters prevent<sup>53</sup> the crossing of the chains.

Some limitations of the model merit discussion. The effect of the solvent on the electrostatic interactions is taken into account implicitly through the dielectric constant  $\epsilon$ . The change in local dielectric properties as well as polarization effects are therefore neglected. The interaction of the surface with the solvent and the polyion is purely electrostatic and there is no short-range attraction, which implies that the interfacial tensions between the surface and solvent and between the surface and polyion beads are similar. The surface in the simulations is assumed to be a nonconducting surface with a dielectric constant identical to the solution. In general, surfaces consist of low dielectric constant materials, and polar solvents near such surfaces give rise to like image charges. These effects are not taken into account in this work.

**B. Simulation Method.** The simulation cell is a cubic box of side length  $L = 16\sigma$  with periodic boundary conditions in the  $x$  and  $y$  directions and surfaces in the  $z$  direction. The system consists of a single polymer chain with  $N = 16$  sites,  $N_{\text{ctr}} = 16$  counterions to balance the charge on the polyion, and  $N_{\text{coi}}$  co-ions to balance the surface charge, with  $N_{\text{coi}} = 16 \times 16\sigma^2\sigma_{\text{SCD}}$ . The monomer density  $\rho_m\sigma^3 \equiv N\sigma^3/L^3$  is approximately 0.004, and the total site density in the simulation cell,  $\rho_{\text{tot}}\sigma^3 \equiv (N + N_{\text{ctr}} + N_{\text{coi}} + N_s)\sigma^3/L^3 = 0.864$ . The polyion, counterions, and co-ions are added first, and then the required number of  $N_s$  solvent molecules are added

so that  $\rho_{\text{tot}}\sigma^3 = 0.864$ . Lengths are measured in units of  $\sigma$ , time in units of  $\tau_{\text{MD}} = (m\sigma^2/\epsilon_{\text{LJ}})^{1/2}$ , and temperature in units of  $\epsilon_{\text{LJ}}/k_B$ . In this calculation we set all three parameters  $m$ ,  $\sigma$ , and  $\epsilon_{\text{LJ}}$  to unity, and a reduced temperature is defined as  $T^* \equiv k_B T/\epsilon_{\text{LJ}}$  which is set to 1.

Initial configurations are generated with the atoms on the lattice points of a face centered cubic structure with  $N_m$  adjacent vertices chosen for the polyion. Initial velocities are generated using a Gaussian random number generator and scaled to the desired temperature. The system is propagated in the canonical ensemble (NVT constant) using an explicit reversible integrator,<sup>54</sup> and the temperature is maintained constant using a Nose-Hoover thermostat.<sup>55,56</sup> An integration time step of  $0.005\tau_{\text{MD}}$  is used, and the Nose-Hoover coupling constant is set to 5. First the system is equilibrated without the charge on the surface, and then the surface charge is switched on and the required number of solvent molecules are converted to co-ions to balance the charge on the surface. The system is then re-equilibrated before properties are averaged. The data are obtained by averaging over 4–6 trajectories, and each trajectory is run for approximately 1 million time steps.

### III. Results and Discussion

**A. Static Properties.** The adsorption behavior of the chain demonstrates an interesting interplay between solvent quality and surface charge density. As expected, increasing the surface charge density promotes adsorption of the polymer chain. Decreasing the solvent quality also promotes adsorption but, in addition, promotes chain collapse. These effects can be quantified via the components of the mean-square radius of gyration parallel and perpendicular to the surface, denoted  $R_{\text{g,para}}^2$  and  $R_{\text{g,perp}}^2$ , respectively, and the molecular axis orientational correlation function  $G_2$ . These quantities are defined as

$$R_{\text{g,para}}^2 = \frac{1}{N} \left\langle \sum_{i=1}^N (x_i - x_{\text{cm}})^2 + (y_i - y_{\text{cm}})^2 \right\rangle \quad (6)$$

$$R_{\text{g,perp}}^2 = \frac{1}{N} \left\langle \sum_{i=1}^N (z_i - z_{\text{cm}})^2 \right\rangle \quad (7)$$

where  $x_i$ ,  $y_i$ , and  $z_i$  are the Cartesian coordinates of the monomer  $i$ , and the subscript  $\text{cm}$  stands for the center of mass of the polyion chain, and

$$G_2 = (3\langle \cos^2\gamma \rangle - 1)/2 \quad (8)$$

where  $\gamma$  is the angle between the molecular axis and the surface. The molecular axis is defined<sup>57</sup> as the eigenvector corresponding to the smallest eigenvalue of the moment of inertia tensor of the molecule. If the molecular axis aligns parallel to the surface, then  $G_2 = -0.5$ ; if it is perpendicular to the surface, then  $G_2 = 1.0$ ; and if it is isotropic, then  $G_2 = 0$ .

For a given solvent quality, increasing the surface charge density causes the chain to adsorb flat on the charged surface, and this is manifested in a decrease in  $G_2$  and  $R_{\text{g,perp}}^2$ . Figure 1 depicts  $G_2$  as a function of  $\sigma_{\text{SCD}}^* (= \sigma_{\text{SCD}}\sigma^2/e)$  for  $\lambda = 0$

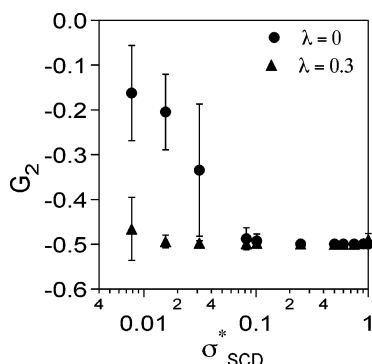


**Figure 1.** Orientation of the polyion plotted as a function of surface charge density,  $\sigma_{\text{SCD}}^*$  for  $\lambda = 0.0$  and  $0.3$ .

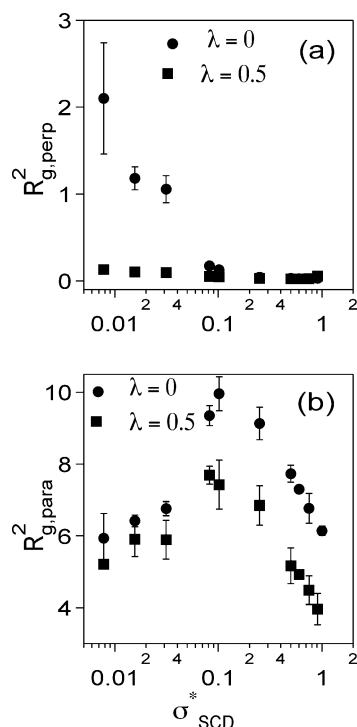


**Figure 2.** Averaged mean square radius of gyration of the polyion perpendicular to the surface,  $R_{\text{g,perp}}^2$ , and parallel to the surface,  $R_{\text{g,para}}^2$ , as a function of surface charge density,  $\sigma_{\text{SCD}}^*$ , for  $\lambda = 0$  and  $0.5$ .

and  $0.3$ . In good solvents ( $\lambda = 0$ ) and for low values of  $\sigma_{\text{SCD}}^*$ , the polyion adopts an almost isotropic orientation near the surface, although it is still slightly biased parallel to the surface, i.e.,  $G_2 < 0$ . As  $\sigma_{\text{SCD}}^*$  is increased, the polyion adsorbs to the surface and for  $\sigma_{\text{SCD}}^* \approx 0.1$  the orientation is completely parallel to the surface ( $G_2 \approx -0.5$ ). When the solvent quality is slightly poor ( $\lambda = 0.3$ ) the polyion is adsorbed flat on the surface even for low values of  $\sigma_{\text{SCD}}^*$  because of the unfavorable monomer–solvent interaction. This behavior is consistent with recent experiments that investigated the size of an adsorbed polyelectrolyte layer exposed to solvents of varying quality<sup>46</sup> where the size of the adsorbed polyelectrolyte layer decreased as the solvent quality was decreased.

Figure 2 depicts  $R_{\text{g,perp}}^2$  and  $R_{\text{g,para}}^2$  as a function of  $\sigma_{\text{SCD}}^*$  for  $\lambda = 0$  and  $0.5$ . The variation of  $R_{\text{g,perp}}^2$  as a function of  $\sigma_{\text{SCD}}^*$  reflects that of  $G_2$  discussed earlier, i.e., as the surface

charge density is increased the chain adsorbs flat onto the surface resulting in a sharp decrease in  $R_{\text{g,perp}}^2$ . Note that for  $\lambda = 0.5$ , the chain is strongly adsorbed on the surface even for  $\sigma_{\text{SCD}}^*$  close to zero. On the other hand, for a given value of  $\lambda$ ,  $R_{\text{g,para}}^2$  displays a nonmonotonic dependence on  $\sigma_{\text{SCD}}^*$ , i.e.,  $R_{\text{g,para}}^2$  increases until the chain is completely flat on the surface, which occurs for  $\sigma_{\text{SCD}}^* \approx 0.1$ , and then begins to decrease. The increase in  $R_{\text{g,para}}^2$  with  $\sigma_{\text{SCD}}^*$  can be explained by noting that the polyion is being confined from three dimensions to two dimensions. The decrease in  $R_{\text{g,para}}^2$  for large values of  $\sigma_{\text{SCD}}^*$  can be explained in terms of the effect of co-ions (counterions to the surface). As  $\sigma_{\text{SCD}}^*$  increases the number of co-ions in the system also increases, and these are found preferentially near the charged surface. This can be seen in snapshots of configurations or density profiles (not shown). Since the co-ions and the polyion are similarly charged, the repulsion from the co-ions results in a decrease in the size of the polyion.

These results are different from previous simulations for polyelectrolytes in good solvents. Lattice simulations<sup>26</sup> found that  $R_{\text{g,para}}^2$  was relatively insensitive to  $\sigma_{\text{SCD}}^*$  although the behavior of  $R_{\text{g,perp}}^2$  was similar to what is seen in this work. In the off-lattice Monte Carlo simulations of Kong and Muthukumar<sup>27</sup> and in the brownian dynamics simulations by Panwar and Kumar<sup>43</sup>  $R_{\text{g,para}}^2$  increased monotonically and  $R_{\text{g,perp}}^2$  decreased monotonically as  $\sigma_{\text{SCD}}^*$  was increased. These differences can be attributed to the neglect of co-ions in previous simulations. If the effect of poor solvent and co-ions is not incorporated, then the adsorption behavior of a polyelectrolyte chain is identical<sup>58,59</sup> to the behavior of neutral polymer chains adsorbed on a surface (as a function of adsorption energy).

For some values of the surface charge density,  $R_{\text{g,perp}}^2$  is a nonmonotonic function of solvent quality. Figure 3 depicts  $R_{\text{g,perp}}^2$  and  $R_{\text{g,para}}^2$  as a function of  $\lambda$  for  $\sigma_{\text{SCD}}^* = 0.1$  and  $0.6$ .  $R_{\text{g,para}}^2$  is a monotonically decreasing function of  $\lambda$  in all cases which is expected because the chain becomes more compact as the solvent quality is decreased. For  $\sigma_{\text{SCD}}^* = 0.1$ ,  $R_{\text{g,perp}}^2$  is a nonmonotonic function of  $\sigma_{\text{SCD}}^*$ . The decrease in  $R_{\text{g,perp}}^2$  occurs because the polyion collapses onto the surface to avoid the unfavorable monomer–solvent interactions. As  $\lambda$  is increased further, however, the attraction between the monomers overcomes the attraction between the surface and the monomers, and this causes the polyion to form a globule instead of a pancake. This does not happen when the monomer–surface interactions are very strong, which is the case for  $\sigma_{\text{SCD}}^* = 0.6$ . These simulations confirm the assumptions of the scaling theory of Borisov<sup>15</sup> et al. where they assumed that the polyion in poor solvent is adsorbed as a pancake structure when  $\sigma_{\text{SCD}}^*$  is high but adopts a hemispherical shape when  $\sigma_{\text{SCD}}^*$  is low. The results from the scaling theory of Borisov<sup>8</sup> et al. for the behavior of single chain near a charged surface cannot be confirmed from these simulations because of the small size of the polyion chain.

**B. Dynamic Properties.** The rotational and translational dynamics of the polyion become *faster* as the solvent quality is decreased, for a given value of the surface charge density. Figure 4(a),(b) depicts the mean-square displacement parallel



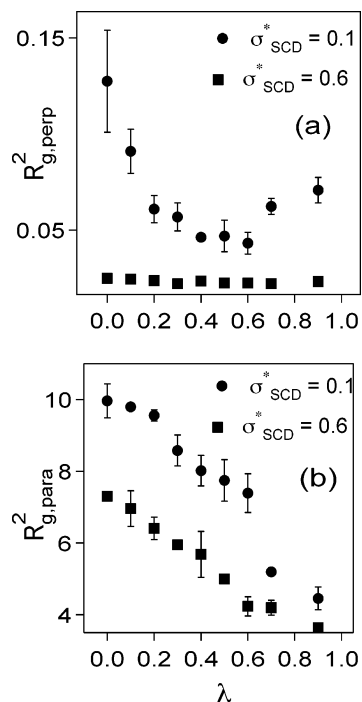


**Figure 3.** Averaged mean square radius of gyration of the polyion perpendicular to the surface,  $R_{g,perp}^2$ , and parallel to the surface,  $R_{g,para}^2$ , plotted as a function of solvent quality,  $\lambda$  for  $\sigma_{SCD}^* = 0.1$  and 0.6.

to the surface (on a log–log plot) and end-to-end vector correlation function as a function of time for  $\sigma_{SCD}^* = 1.5$  and  $\lambda = 0, 0.3$ , and 0.5. MSD is the mean-square displacement of the center of mass of the adsorbed polyion chain parallel to the surface, i.e.,  $MSD = \langle |\mathbf{R}_{||}(t) - \mathbf{R}_{||}(0)|^2 \rangle$ , and the lateral diffusion coefficient,  $D_{||}$ , is defined via  $\langle |\mathbf{R}_{||}(t) - \mathbf{R}_{||}(0)|^2 \rangle = 4D_{||}t$ , where  $\mathbf{R}_{||}(t) = x_{cm}(t)\hat{i} + y_{cm}(t)\hat{j}$ . The end-to-end vector autocorrelation function,  $C(t)$  is defined as  $C(t) = \langle \mathbf{R}(0) \cdot \mathbf{R}(t) \rangle / \langle \mathbf{R}^2(0) \rangle$  where  $\mathbf{R}(t)$  is the end-to-end vector of the chain at time  $t$ . In all cases the center of mass of the polyion shows subdiffusive behavior at shorter time scales and normal lateral diffusion at a longer time scale, i.e., MSD is a linear function of time. The crossover time from subdiffusive to normal diffusion decreases as the solvent quality is decreased. And as the solvent quality is decreased, the translational diffusion is faster, i.e.,  $D_{||}$  increases, taking on values (in units of  $\sigma^2/\tau_{MD}$ ) of  $4.52 \times 10^{-3}$ ,  $4.93 \times 10^{-3}$ , and  $7.57 \times 10^{-3}$  (statistical uncertainties are in the last significant digit) for  $\lambda = 0, 0.3$ , and 0.5. The faster translational diffusion is accompanied by faster rotation. For  $\lambda = 0$ ,  $C(t)$  does not decay over the course of the simulation, but the decay becomes faster as the solvent quality is decreased.

We characterize the rotational relaxation via the initial (short time) decay of  $C(t)$ . At short times, i.e.,  $t \leq 200\tau_{MD}$ , the decay of  $C(t)$  is well-fit by a single exponential, and we define a relaxation time  $\tau$  as the time constant of this exponential. We are unable to reliably extract the long time relaxation behavior because  $C(t)$  does not decay in some cases and in others the statistics are poor even with trajectories of length  $5000\tau_{MD}$ . The rotational relaxation time  $\tau$  for  $\sigma_{SCD}^* = 1.5$  shown in Figure 4(b) takes on values of (in

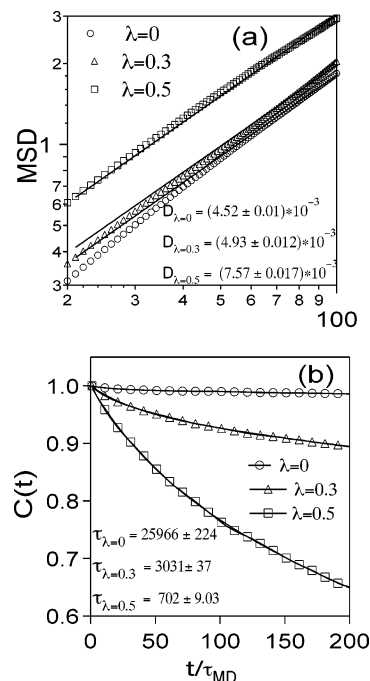


**Figure 4.** (a) Log–log plot of the lateral mean-square displacement of the center of mass of the polyion versus time for  $\sigma_{SCD}^* = 1.5$ . Solid lines are fit to the data. (b) End-to-end time autocorrelation function plotted versus time for  $\sigma_{SCD}^* = 1.5$ . Solid lines are fit to the data, and it overlaps with the line of the markers.

units of  $\tau_{MD}$ )  $25\,966 \pm 224$ ,  $3031 \pm 37$ , and  $702 \pm 9$  for  $\lambda = 0, 0.3$ , and 0.5, respectively.

An interesting feature from Figure 4 is that although  $C(t)$  does not decay for some values of  $\lambda$ , the chain exhibits normal center-of-mass diffusion. This decoupling of rotational and translational dynamics is often viewed as a signature of “glassy” behavior, since it is reminiscent of what is observed in the dynamics of supercooled liquids. It has been suggested<sup>60–63</sup> that the strong interactions between a polymer and the surface can result in the polyion becoming trapped in local minima. In the present work the behavior exhibited by the polyion is not due to the interaction of the polyion with the surface but rather because of the interaction between the polymer and the solvent.

There are several possible explanations for the faster dynamics as the solvent quality is decreased. First of all, as the solvent is made poorer, the hydrodynamic radius decreases, and this can result in an increase in the diffusion coefficient. Another possibility is that this is caused by the confinement of the chain from three dimensions to two dimensions, and the dynamics of two-dimensional chains are expected to be faster than three-dimensional chains. Finally, as the solvent quality is decreased the density of the solvent molecules near the surface decreases, and this results in a lower friction on the adsorbed chain.

Figure 5(a),(b) depicts the total density of sites and the solvent density as a function of distance from the charged surface. As the solvent quality is decreased the solvent density near the surface decreases. This is not very prominent in Figure 5(a) but is more clearly seen in Figure 5(b) where the value of the peak near  $z = 2$  decreases by about 75%

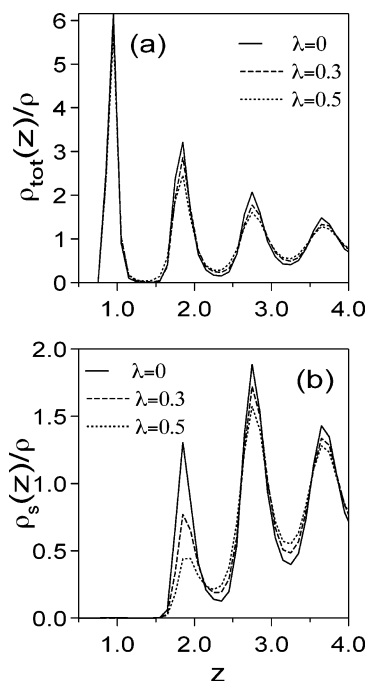


**Figure 5.** (a) Total density profile of the species as a function of the distance from the surface for  $\sigma_{\text{SCD}}^* = 1.5$ . (b) Density profile of the solvent as a function of the distance from the surface for  $\sigma_{\text{SCD}}^* = 1.5$ .

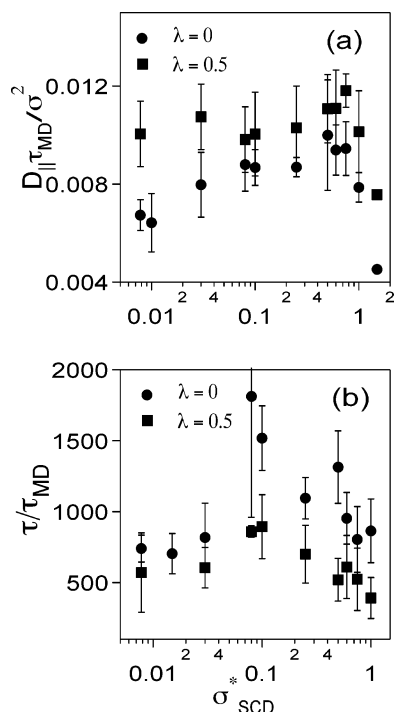


**Figure 6.** (a)  $D_{\parallel}$  plotted as a function of  $\sigma_{\text{SCD}}^*$  for  $\lambda = 0.0$  and  $0.5$ . (b)  $\tau$  plotted as a function of  $\sigma_{\text{SCD}}^*$  for  $\lambda = 0.0$  and  $0.5$ .

for  $\lambda$  going from 0 to 0.5. It is possible that the decrease in site density in the layer adjacent to the polyion results in a weaker friction and therefore faster dynamics of the adsorbed polyion.

The diffusion coefficient and end-to-end vector relaxation time are nonmonotonic functions of the solvent quality in some cases. Figure 6(a),(b) depicts  $D_{\parallel}$  and  $\tau$ , respectively, as a function of  $\sigma_{\text{SCD}}^*$  for  $\lambda = 0$  and  $0.5$ . For  $\lambda = 0$ ,  $D_{\parallel}$  is a

nonmonotonic function of  $\sigma_{\text{SCD}}^*$  with a peak that occurs at a value of  $\sigma_{\text{SCD}}^*$  where the chain is adsorbed flat to the surface. One can attribute the increase in  $D_{\parallel}$  with increasing  $\sigma_{\text{SCD}}^*$  for lower surface charge densities to a confinement of the chain from three to two dimensions and the decrease in  $D_{\parallel}$  with increasing  $\sigma_{\text{SCD}}^*$  for higher surface charge densities to the strong wall-polymer interaction which increases the friction with the surface. For a given  $\sigma_{\text{SCD}}^*$ ,  $D_{\parallel}$  is always higher in poorer solvents. This is because the chain size is smaller and the solvent density at the surface is lower as the solvent quality is decreased, both of which tend to increase  $D_{\parallel}$ . In poorer solvents, however,  $D_{\parallel}$  is relatively insensitive to the surface charge density (within statistical uncertainties) because the polyion is always adsorbed completely on the surface for all surface charge densities. For both  $\lambda = 0$  and  $0.5$   $\tau$  is a nonmonotonic function of  $\sigma_{\text{SCD}}^*$  with a peak at approximately  $\sigma_{\text{SCD}}^* \approx 0.1$  which is when the polyion is completely adsorbed to the surface. Again the effect of changing the surface charge is more significant in good solvents than in poor solvents. One can attribute the increase in  $\tau$  for low values of  $\sigma_{\text{SCD}}^*$  to a confinement of the chain from three to two dimensions. The decrease in  $\tau$  for  $\sigma_{\text{SCD}}^*$  greater than 0.1 can be due to the decrease in size of polyion which will facilitate the rotation of the polyion on the surface leading to a smaller  $\tau$ .

#### IV. Conclusions

The static and dynamic properties of a single charged chain near a planar charged surface are studied using molecular dynamics simulation with explicit solvent. The properties of an adsorbed chain can be very different depending on the solvent quality. The chain is adsorbed parallel to the surface when the solvent is poor enough, independent of the surface charge, unlike in good solvents where the surface charge plays a dominant role. Interestingly the dynamics of the chain become faster as the solvent quality is decreased, which could be either due to the lower solvent density at the surface or due to the confinement of the chain to two dimensions.

#### References

- (1) Forster, S.; Schmidt, M. *Adv. Polym. Sci.* **1995**, *13*, 51.
- (2) Holm, C.; Joanny, J.; Kremer, K.; Netz, R.; Reineker, P.; Seidel, C.; Vilgis, T.; Winkler, R. *Adv. Polym. Sci.* **2004**, *166*, 67.
- (3) Barrat, J.; Joanny, J. *Adv. Chem. Phys.* **1996**, *94*, 1.
- (4) Netz, R.; Andelman, D. *Phys. Rep.* **2003**, *380*, 1.
- (5) Wiegand, F. *J. Phys. A: Math. Gen.* **1977**, *10*, 299.
- (6) Muthukumar, M. *J. Chem. Phys.* **1987**, *86*, 7230.
- (7) Varoqui, R. *J. Phys. II Fr.* **1993**, *3*, 1097.
- (8) Borisov, O.; Zhulina, E.; Birshtein, T. *J. Phys. II Fr.* **1994**, *4*, 913.
- (9) Chatellier, X.; Senden, T.; Joanny, J.; di Meglio, J. *Europhys. Lett.* **1998**, *41*, 303.
- (10) Netz, R.; Joanny, J. *Macromolecules* **1999**, *32*, 9013.
- (11) Joanny, J. *Euro. Phys. J. B* **1999**, *9*, 117.
- (12) Dobrynin, A.; Deshpande, A.; Rubinstein, M. *Phys. Rev. Lett.* **2000**, *84*, 3101.

- (13) Dobrynin, A.; Deshkovski, A.; Rubinstein, M. *Macromolecules* **2001**, *34*, 3421.
- (14) Dobrynin, A. *J. Chem. Phys.* **2001**, *114*, 8145.
- (15) Borisov, O.; Hakem, F.; Vilgis, T.; Joanny, J.; Johner, A. *Euro. Phys. J. E* **2001**, *6*, 37.
- (16) Dobrynin, A.; Rubinstein, M. *Macromolecules* **2002**, *35*, 2754.
- (17) Dobrynin, A.; Rubinstein, M. *J. Phys. Chem. B* **2003**, *107*, 8260.
- (18) Linse, P. *Macromolecules* **1996**, *29*, 326.
- (19) Chatellier, X.; Joanny, J. *J. Phys. II Fr.* **1996**, *6*, 1669.
- (20) Borukhov, I.; Andelman, D. *Macromolecules* **1998**, *31*, 1665.
- (21) Park, S.; Barrett, C.; Rubner, M.; Mayes, A. *Macromolecules* **2001**, *34*, 3384.
- (22) Shafir, A.; Andelman, D.; Netz, R. *J. Chem. Phys.* **2003**, *119*, 2355.
- (23) Cheng, H.; Olvera de la Cruz, M. *J. Chem. Phys.* **2003**, *119*, 12635.
- (24) Patra, C.; Chang, R.; Yethiraj, A. *J. Phys. Chem. B* **2004**, *108*, 9126.
- (25) Shafir, A.; Andelman, D. *Phys. Rev. E* **2004**, *70*, 061804.
- (26) Beltran, S.; Hooper, H.; Blanch, H.; Prausnitz, J. *Macromolecules* **1991**, *24*, 3178.
- (27) Kong, C.; Muthukumar, M. *J. Chem. Phys.* **1998**, *109*, 1522.
- (28) Ellis, M.; Kong, C.; Muthukumar, M. *J. Chem. Phys.* **2000**, *112*, 8723.
- (29) McNamara, J.; Kong, C.; Muthukumar, M. *J. Chem. Phys.* **2002**, *117*, 5354.
- (30) Yamakov, V.; Milchev, A.; Borisov, O.; Dunweg, B. *J. Phys. Condens. Matter* **1999**, *11*, 9907.
- (31) Messina, R. *Phys. Rev. E* **2004**, *70*, 051802.
- (32) Chodanowski, P.; Stoll, S. *J. Chem. Phys.* **2001**, *115*, 4951.
- (33) Chodanowski, P.; Stoll, S. *Macromolecules* **2001**, *34*, 2320.
- (34) Stoll, S.; Chodanowski, P. *Macromolecules* **2002**, *35*, 9556.
- (35) Messina, R.; Holm, C.; Kremer, K. *Langmuir* **2003**, *19*, 4473.
- (36) Messina, R.; Holm, C.; Kremer, K. *Phys. Rev. E* **2002**, *65*, 041805.
- (37) Messina, R.; Holm, C.; Kremer, K. *J. Chem. Phys.* **2002**, *117*, 2947.
- (38) Messina, R. *J. Chem. Phys.* **2003**, *119*, 8133.
- (39) Messina, R.; Holm, C.; Kremer, K. *J. Polym. Sci. Part B: Polym. Phys.* **2004**, *42*, 3557.
- (40) Messina, R. *Macromolecules* **2004**, *37*, 621.
- (41) Panchagnula, V.; Jeon, J.; Dobrynin, A. *Phys. Rev. Lett.* **2004**, *93*, 037801.
- (42) Panchagnula, V.; Jeon, J.; Rusling, J.; Dobrynin, A. *Langmuir* **2005**, *21*, 1118.
- (43) Panwar, A.; Kumar, S. *J. Chem. Phys.* **2005**, *122*, 154902.
- (44) Wang, X. L.; Lu, Z. Y.; Li, Z. S.; Sun, C. C. *J. Phys. Chem. B* **2005**, *109*, 17644.
- (45) Dubas, S. T.; Schlenoff, J. B. *Macromolecules* **1999**, *32*, 8153.
- (46) Poptoshev, E.; Schoeler, B.; Caruso, F. *Langmuir* **2004**, *20*, 829.
- (47) Kotov, N. *Nanostruct. Mater.* **1999**, *12*, 789.
- (48) Hill, T. L. *An Introduction to Statistical Thermodynamics*; Dover: New York, 1960.
- (49) Chang, R.; Yethiraj, A. *J. Chem. Phys.* **2001**, *114*, 7688.
- (50) Chang, R.; Yethiraj, A. *J. Chem. Phys.* **2003**, *118*, 6634.
- (51) Bitsanis, I.; Hadziioannou, G. *J. Chem. Phys.* **1990**, *92*, 3827.
- (52) Feynman, R. P.; Leighton, R. B.; Sands, M. *The Feynman Lectures on Physics*; Addison-Wesley: Reading, 1964; Vol. 2.
- (53) Grest, G.; Kremer, K. *Phys. Rev. A* **1986**, *33*, 3628.
- (54) Tuckerman, M.; Berne, B. J.; Martyna, G. J. *J. Chem. Phys.* **1992**, *97*, 1990.
- (55) Nose, S. *J. Chem. Phys.* **1984**, *81*, 511.
- (56) Hoover, W. G. *Phys. Rev. A* **1985**, *31*, 1695.
- (57) Yethiraj, A. *Adv. Chem. Phys.* **2002**, *121*, 89.
- (58) Milchev, A.; Binder, K. *Macromolecules* **1996**, *29*, 343.
- (59) Lai, P.-Y. *Phys. Rev. E* **1994**, *49*, 5420.
- (60) Mansfield, K. F.; Theodorou, D. N. *Macromolecules* **1989**, *22*, 3143.
- (61) Chakraborty, A. K.; Sha\_er, J. S.; Adriani, P. M. *Macromolecules* **1991**, *24*, 5226.
- (62) Chakraborty, A. K.; Adriani, P. M. *Macromolecules* **1992**, *25*, 2470.
- (63) Smith, G. D.; Bedrov, D.; Borodin, O. *Phys. Rev. Lett.* **2004**, *70*, 051802.

CT050267U